LEVEL II

SC5271.3SA

SC5271.3SA

Copy No. ___5___

NUMERICAL METHODS
FOR 2-DIMENSIONAL MODELING

W. D. Murphy and W. F. Hall
Rockwell International Science Center
P. O. Box 1085
Thousand Oaks, California 91360

December, 1980

Semi Annual Technical Report No. 1
for Period 1 July 1980 – 31 December 1980

Approved for public release; distribution unlimited.

The views and conclusions contained in this document are
those of the authors and should not be interpreted as
representing the official policies, either expressed or
implied, of the Defense Advanced Research Projects
Agency of the U.S. Government.

DTIC
ELECTE
S
JAN 1 4 1981
D

A

Rockwell International
Science Center

81 1 13 016

REPORT DOCUMENTATION PAGE	READ INSTRUCTIONS BEFORE COMPLETING FORM

1. REPORT NUMBER	2. GOVT ACCESSION NO. AD-A093843	3. RECIPIENT'S CATALOG NUMBER

4. TITLE (and Subtitle) NUMERICAL METHODS FOR 2-DIMENSIONAL MODELING.	5. TYPE OF REPORT & PERIOD COVERED Semi-Annual Technical Report 1 J. -31
	6. PERFORMING ORG. REPORT NUMBER SC5271.3SA

7. AUTHOR(s) W.D. Murphy and W.F. Hall	8. CONTRACT OR GRANT NUMBER(s) MDA903-80-C-0498 DARPA Order-3984

9. PERFORMING ORGANIZATION NAME AND ADDRESS Rockwell International Science Center P.O. Box 1085 Thousand Oaks, California 91360	10. PROGRAM ELEMENT, PROJECT, TASK AREA & WORK UNIT NUMBERS DARPA Order No. 3984

11. CONTROLLING OFFICE NAME AND ADDRESS Defense Advanced Research Project Agency 1400 Wilson Boulevard Arlington, Virginia 22209 (TIO/Admin.)	12. REPORT DATE December, 1980
	13. NUMBER OF PAGES 36

14. MONITORING AGENCY NAME & ADDRESS(if different from Controlling Office) Department of the Army Defense Supply Service-Washington Washington, D.C. 20310	15. SECURITY CLASS. (of this report) Unclassified
	15a. DECLASSIFICATION/DOWNGRADING SCHEDULE

16. DISTRIBUTION STATEMENT (of this Report)

Approved for public release; distribution unlimited

17. DISTRIBUTION STATEMENT (of the abstract entered in Block 20, if different from Report)

18. SUPPLEMENTARY NOTES

19. KEY WORDS (Continue on reverse side if necessary and identify by block number)

very large scale integration (VLSI), diffusion, solid state, electron devices

20. ABSTRACT (Continue on reverse side if necessary and identify by block number)

Progress toward the development of a fast algorithm for two-dimensional computational modeling of VLSI fabrication processes is described. The first report of an algorithm producing two-dimensional dopant profiles in seconds per process step is presented. A summary of investigations to date and plans for future work are discussed.

DD FORM 1473 EDITION OF 1 NOV 65 IS OBSOLETE
1 JAN 73

389949

CONTENTS

ILLUSTRATIONS

iii

TABLES

1.0 SUMMARY

This technical report presents the results and progress
of the first six months of research on numerical methods for
two-dimensional process modeling under Contract MDA903-80-C-0498,
DARPA Order No. 3984. A significant milestone has been passed
in this initial period, well in advance of our anticipated
schedule: An algorithm of sufficient speed to be used for
routine VLSI process modeling has been found. It is orders
of magnitude faster than methods presently being used in the
U.S. and abroad, requiring only seconds per process step on
the CDC Cyber 176 to generate full two-dimensional detail on
dopant spread. A description of the algorithm will be found
in Section 3.2 below.

1.1 TASK OBJECTIVES

The overall objective of this program is to develop fast
and accurate methods for computer modeling of the two-
dimensional spread of dopants and other defects during VLSI
circuit fabrication. Our initial goals are to demonstrate
these methods for nonlinear diffusion of a single dopant
during oxide growth, and to provide the resulting computa-
tional algorithms in a form suitable for incorporation into
a general process modeling computer code, such as Stanford's
program SUPREM.

Three tasks have been defined for the first year's effort:

Task 1 — Analysis of Numerical Methods

Task 2 — Formulation of Test Cases

Task 3 — Algorithm Development and Evaluation .

Their objectives are, respectively:

Task 1 — Select promising algorithms from other disciplines, primarily fluid dynamics, where considerable progress on numerical methods for multidimensional problems has recently been made.

Task 2 — a) Determine realistic parameter ranges to be used as test cases for source and drain diffusion into a short MOSFET channel region.

b) Develop and analyze two-dimensional diffusion problems for which dopant profiles can be obtained to high accuracy by existing techniques.

Task 3 — a) Evaluate each selected algorithm for speed and accuracy.

b) Adapt the most promising algorithm(s) to solve the combined oxidation-nonlinear diffusion problem for a single dopant species in two dimensions.

1.2 TECHNICAL PROBLEM

The fabrication of VLSI devices requires production of features of submicron size and separation. Electrical characteristics such as threshold and punchthrough voltages will be sensitive to dopant spread into critical areas adjacent to the original features. Experimental control of this spreading, without guidance from accurate computer modeling, will be costly, tedious, and time-consuming. However, the use of standard numerical methods to achieve an adequate

modeling capability is also costly and time-consuming. One
should therefore seek advanced methods, drawn from areas
such as fluid dynamics, where considerable effort and
ingenuity have been expended in recent years to develop fast
and accurate solvers for the characterization of multidimen-
sional, time-dependent phenomena.

1.3 GENERAL METHODOLOGY

Based upon our own ongoing research in computational
nonlinear aerodynamics, we have identified several promising
approaches to the development of a fast solver for two-
dimensional diffusion problems. After a preliminary screen-
ing, a few of these have been selected for adaptation to the
problem of dopant spread during oxidation or annealing. These
algorithms will be tested for speed and accuracy on the prob-
lem of nonlinear dopant diffusion into the channel region of
a MOSFET, as well as on simpler problems for which the actual
dopant profiles can be accurately obtained by other means.

1.4 TECHNICAL RESULTS

Two algorithms have gone through preliminary screening:
high-order finite element methods, and a multidimensional
version of the method of lines, both utilizing an optimized
stiff integrator for the time integration. The finite element
methods have proved disappointing, but the method of lines
has provided an unexpectedly large gain in speed. Two-
dimensional post-annealing profiles (without oxidation) for
a 15-minute drive-in cycle on boron-implanted silicon at
1100°C, with a peak initial boron concentration of 10^{20} cm^{-3},
were obtained in ten seconds of CPU time on the Cyber 176.

These results can be directly compared with the recently published work of Warner and Wilson (Bell System Tech. J. 59, 1 (1980)), where similar nonlinear diffusion problems with the same number of unknowns (a 21×41 grid), solved by second-order finite element methods, took over seven minutes on the Cray-1 computer, a machine which is five to fifteen times faster than the Cyber 176. Comparing equivalent CPU times on the Cyber 176, one finds our method of lines algorithm to be at least two orders of magnitude faster than the algorithm used by Warner and Wilson. A more detailed discussion of these results can be found in Sections 3.2 and 3.3.

1.5 IMPORTANT FINDINGS AND CONCLUSIONS

The speed of the method of lines algorithm is already sufficient to render its use for routine process design practical for a process engineer with access to the latest IBM or CDC computers. Since these machines can currently be rented economically on a time-sharing basis, it appears that we now have in hand the core of a new two-dimensional process simulator. Our immediate priorities should therefore be to complete the testing and characterization of this algorithm, and to extend its use to diffusion during oxidizing process cycles, where the oxide-silicon boundary moves nonuniformly.

1.6 SPECIAL COMMENTS

To facilitate the transfer of this algorithm into a complete, two-dimensional process simulator, an early meeting

with researchers at Stanford responsible for simulator
development has been tentatively scheduled for March, 1981.
By this date, good measures of the overall performance of
the method of lines algorithm will have been obtained.

1.7 IMPLICATIONS FOR FURTHER RESEARCH

The work of testing potentially fast algorithms for
multidimensional VLSI problems has barely begun. There
remain at least two strong motivations to continue research
on new methods: to find methods which can be applied
economically to derive VLSI device electrical characteristics
from two-dimensional dopant profiles, and to extend the
treatment of device structure formation to the level of
the actual defect processes, involving multispecies migration
and chemical reaction. This will ultimately provide a better
bridge from the physics of solid-state defect dynamics to
the engineering observables than the current, semi-empirical
models. Such a tool can be used to recalibrate these models
for new situations, and to determine at what scale new
effects will appear and become important to device performance.

1.8 ORGANIZATION OF THE REPORT

The basic formulation of the equations describing one-
dimensional nonlinear diffusion, with segregation at a moving
oxide-silicon boundary, is given in Section 2.1. This is
followed by a presentation of the two numerical procedures
examined to date (Section 2.2) and a summary of results for
one-dimensional test cases (Section 2.3).

In Section 3, the generalization of these problems to
two dimensions is considered. For the reasons stated in
Section 3.2, two-dimensional numerical tests have only been
carried out on the method of lines algorithm. Alternative
approaches to the treatment of the nonuniformly moving oxide-
silicon boundary are described in Section 3.1. Results for
a nonmoving, planar boundary are presented in Section 3.3.
Plans for future work are outlined in Section 4.

2.0 ONE-DIMENSIONAL REDISTRIBUTION PROBLEMS

Initial computations were carried out on one-dimensional redistribution problems to keep computer costs low, to learn the limitations of the various numerical procedures, and to determine the number of grid points required to obtain satisfactory resolution.

2.1 MATHEMATICAL FORMULATION

The redistribution of impurities in silicon-on-sapphire (SOS)-type structures during thermal oxidation was treated by Maldonado and Murphy[1] as a nonlinear diffusion equation with a moving boundary. This equation can be transformed to one having a fixed boundary by introducing the change of variables

$$\xi = (x - mU(t)) L_I / L(t) \tag{1a}$$

$$\tau = t \tag{1b}$$

where m is the ratio of the thickness of silicon consumed, given by $L(0) - L(t)$, to the oxide thickness, $U(t)$. L_I represents a characteristic length at $t = 0$, which is given by $L_I = L(0) - mU(0)$ and denotes the right boundary. In these new variables the governing equation for the impurity concentration, $N(\xi, \tau)$, is given by

$$\frac{\partial N(\xi, \tau)}{\partial \tau} = \left[\frac{L_I}{L(\tau)} \right]^2 \frac{\partial}{\partial \xi} \left\{ D\left[N(\xi, \tau) \right] \frac{\partial N(\xi, \tau)}{\partial \xi} \right\}$$
$$+ (L_I - \xi) \frac{m\dot{U}(\tau)}{L(\tau)} \frac{\partial N(\xi, \tau)}{\partial \xi} \tag{2a}$$

7

with boundary conditions

$$\frac{\partial N(0,\tau)}{\partial \tau} = \frac{L(\tau)}{L_I} \ (k-m) \ \frac{\dot{U}(\tau)N(0,\tau)}{D(N(0,\tau))} \tag{2b}$$

$$\frac{\partial N(L_I,\tau)}{\partial \xi} = 0 \tag{2c}$$

and initial condition

$$N(\xi,0) = N^0(\xi) \ . \tag{2d}$$

k is the segregation coefficient, and $N^0(\xi)$ is usually selected as a Gaussian, modeling the type of doping profile which results from ion implantation. The nonlinear diffusion function is[1]

$$D(N) = D^0 \left[N + \frac{N^2 + 2n_{in}^2}{(N^2 + 4n_{in}^2)^{\frac{1}{2}}} \right] \frac{1}{n_{in}} \tag{2e}$$

where n_{in} is the intrinsic carrier density at the given process temperature and D^0 is the intrinsic diffusivity.

This nonmoving boundary value problem (2) is much easier to solve numerically than the original one proposed by Maldonado and Murphy.[1] In fact, the numerical results to be presented will indicate that good accuracy is achievable using relatively coarse grids when discretizing equation (2).

2.2 NUMERICAL PROCEDURES

2.2.1 B-splines

The Galerkin method using piecewise polynomial B-splines (see deBoor[2]) consists of approximating the concentration by

$$N_s(\xi,\tau) = \sum_{i=1}^{n} \alpha_i(\tau) B_i(\xi) \tag{3}$$

where the $B_i(\xi)$ are known polynomials of order k which vanish outside of specified intervals. If N is replaced by N_s in equation (2) and the resulting expression is multiplied by $B_q(\xi)$ and integrated over $\left|0, L_I\right|$, the Galerkin formulation takes the form

$$\int_0^{L_i} \frac{\partial N_s(\xi,\tau)}{\partial \tau} B_q(\xi) ds = - \left[\frac{L_I}{L(\tau)}\right]^2 \int_0^{L_I} D(N_s) \frac{\partial N_s}{\partial \xi} \frac{dB_q}{d\xi} d\xi$$

$$+ \frac{m\dot{U}(\tau)}{L(\tau)} \int_0^{L_I} (L_I - \xi) \frac{\partial N_s}{\partial \xi} B_q d\xi - \frac{L_I}{L(\tau)} (K - m)\dot{U}(\tau) N_s(0,\tau) B_q(0)$$

$$\tag{4a}$$

$$\int_0^{L_I} N_s(\xi,0) B_q(\xi) d\xi = \int_0^{L_I} N^0(\xi) B_q(\xi) d\xi \tag{4b}$$

$$q = 1, 2, \cdots, n$$

where one integration by parts was applied. Equation (4) may be written in matrix form as the following system of nonlinear initial value ordinary differential equations:

$$A \frac{d\alpha}{d\tau} = F(\alpha, \tau) \tag{5}$$

where $\alpha = (\alpha_1(\tau), \alpha_2(\tau), \cdots, \alpha_n(\tau))^T$,

$A = \left(\int_0^{L_I} B_i(\xi) B_j(\xi) d\xi \right)$, and the initial value $\alpha(0)$ is obtained

from solving equation (4b).

The following numerical characteristics are well known for such problems as (4) and (5):

(1) The matrix A has half bandwidth k-1.

(2) All integrals in equation (4) may be evaluated accurately using k^{th} order Gaussian quadratures between the knots of the B-splines if the separation is sufficiently small.

(3) Equation (5) is stiff (see Gear[3]) and, consequently, stiffly stable integration procedures must be used. This typically requires the evaluation of the Jacobian, $\partial F / \partial \alpha$, which also has half bandwidth equal to k-1.

(4) k^{th} order B-splines lead to numerical approximations, N_s, which are k^{th} order accurate in the spatial discretization parameter.

The time integration of (5) is carried out using a robust integrator with automatic variable step-and-order

10

changes from first to fifth order. Thus, the user need only specify an error tolerance, and the integrator automatically guarantees that the time-integration steps satisfy this criterion. Spatial errors are reduced by increasing the number n of B-splines or increasing their order, k. The motivation for considering such a method is that by employing high order B-splines (large values of k) we might be able to reduce the number n required to provide acceptable accuracy and as a by-product reduce computer time. This must be balanced against any increase in computation caused by the increase in bandwidth of the matrices A and $\partial F/\partial \alpha$.

2.2.2 Method of Lines

We will describe this method by using a uniform mesh $\Delta \xi = L_I/n$ on the interval $\left[0, L_I\right]$, although a nonuniform mesh has been applied, occasionally. The partial differential equation (2a) is discretized in the spatial variable ξ using centered differences; i.e., for $q = 1, 2, \cdots, n-1$,

$$\frac{dN(\xi_q, \tau)}{d\tau} = \left[\frac{L_I}{L(\tau)}\right]^2 \left[\frac{D_{q+\frac{1}{2}}(N_{q+1} - N_q) - D_{q-\frac{1}{2}}(N_q - N_{q-1})}{(\Delta \xi)^2}\right]$$

$$+ (L_I - \xi_q) \frac{m\dot{U}(\tau)}{L(\tau)} \frac{N_{q+1} - N_{q-1}}{2\Delta \xi} \tag{6a}$$

where $\xi_q = q\Delta \xi$, $N_q = N(\xi_q, \tau)$, $N_{q \pm \frac{1}{2}} = \frac{1}{2}(N_{q \pm 1} + N_q)$, and $D_{q \pm \frac{1}{2}} = D(N_{q \pm \frac{1}{2}})$. The boundary conditions are discretized using one-sided differences in (2a), and combining this with (2b) and (2c) yields

11

$$\frac{dN(\xi_0,\tau)}{d\tau} = 2\left[\frac{L_I}{L(\tau)}\right]^2 \left[\frac{D_{\frac{1}{2}}(N_1-N_0)}{(\Delta\xi)^2} - \frac{L(\tau)}{L_I}\frac{(k-m)\dot{U}(\tau)N_0}{\Delta\xi}\right]$$

$$+ m(k-m)\left[\dot{U}(\tau)\right]^2 N_0/D_0 \tag{6b}$$

and

$$\frac{dN(\xi_n,\tau)}{d\tau} = -2\left[\frac{L_I}{L(\tau)}\right]^2 D_{n-\frac{1}{2}}\frac{(N_n-N_{n-1})}{(\Delta\xi)^2} . \tag{6c}$$

Equation (6) may be written in the form

$$\frac{dN_q}{d\tau} = g_q(N_{q-1},N_q,N_{q+1},\tau) \quad , \quad q = 1,2,\cdots,n-1 \tag{7a}$$

$$\frac{dN_0}{d\tau} = g_0(N_0,N_1,\tau) \tag{7b}$$

$$\frac{dN_n}{d\tau} = g_n(N_{n-1},N_n,\tau) \tag{7c}$$

with initial conditions given by

$$N_q(0) = N^0(\xi_q) . \tag{7d}$$

Equation (7) is solved efficiently using a stiff integrator called GEARB developed by Hindmarsh.[4] Note that the Jacobian, $\partial g/\partial N$, is tridiagonal, so that it may be

inverted easily. This integrator is also variable-order and variable-step-size and employs the implicit backward differentiation formulas, which are now quite common for treating stiff ordinary differential equations. Excellent error control is the strong point for this technique.

2.3 NUMERICAL RESULTS

2.3.1 B-splines

For our test case we use an example described by Prince and Schwettmann.[5] This involves the redistribution of a high dose 80 keV boron implant in (111) silicon. The redistribution is done by bringing the silicon into contact with an oxidizing (steam) ambient at 1100°C. This is a highly nonlinear case and contains a highly peaked Gaussian as an initial condition, which is difficult to approximate by an equation of the form (3) when n is relatively small. To alleviate this problem we employ a logarithmic transformation of the form

$$N(\xi,\tau) = e^{u(\xi,\tau)} .$$

In Table 1 below, a list is given of some solution values at the SiO_2-Si interface at time $\tau = 0.75$ hour for various order k and number of uniform subintervals ℓ on a silicon slab of length 2 µm. Here $n = \ell + k - 1$. CPU denotes the running time on the IBM 3033 in minutes and 3.169(18) signifies the number 3.169×10^{18}.

Observe that the CPU time is approximately linear in ℓ but quadratic in k. Also, since the solution ranges over

13

Table 1. Solution Using B-splines

k	ℓ	CPU	u	N
2	50	0.089	42.60	3.169(18)
3	20	0.080	42.70	3.503(18)
3	30	0.117	42.58	3.106(18)
3	50	0.191	42.57	3.076(18)
4	10	0.061	43.17	5.604(18)
4	25	0.222	42.61	3.201(18)
4	50	0.400	42.57	3.076(18)
5	50	0.682	42.57	3.076(18)
6	25	0.578	42.58	3.106(18)
6	50	1.081	42.57	3.076(18)

many orders of magnitude, a certain minimum number of subintervals is required to accurately monitor the redistribution. In this example the third order method (k = 3) employing 30 subintervals is about optimal when both accuracy and computer time are considered. This means that in two dimensions a grid of 30 × 60 points using a third order method should suffice when the lateral dimension is twice the depth (a typical application in MOSFET process design).

2.3.2 Method of Lines

The logarithm transformation needed for high-order B-splines was not required here, since the initial data (7d) is used directly as initial conditions for the ordinary differential equations. In Table 2 we again list some

14

Table 2.   Solution By Method of Lines

n+1	CPU	N
205	0.347	6.039(18)
45	0.107	6.040(18)
21	0.068	6.152(18)

interface values at time τ = 0.75 hour for various numbers of grid points n+1. However, this time we use the SUPREM default values for the parameters in the code, which explains the differences between the surface concentration values in the two tables.

SUPREM gave a value of N = 5.49(18) using 0.076 minute of CPU time. Observe that acceptable accuracy can be achieved with only 21 grid points, which translates to a grid of 21 × 41 in two dimensions.

3.0 TWO-DIMENSIONAL REDISTRIBUTION PROBLEMS

As we have learned by studying one-dimensional problems, the moving boundary problem can be greatly simplified by mapping it into a fixed region. In two dimensions, two different types of mappings into a rectangle are considered: (1) translation-stretching, and (2) conformal mapping.

3.1 FORMULATION

3.1.1 Translation-Stretching

In Figure 1 below is a model for the field oxidation step in the fabrication of an MOS device in physical coordinates.
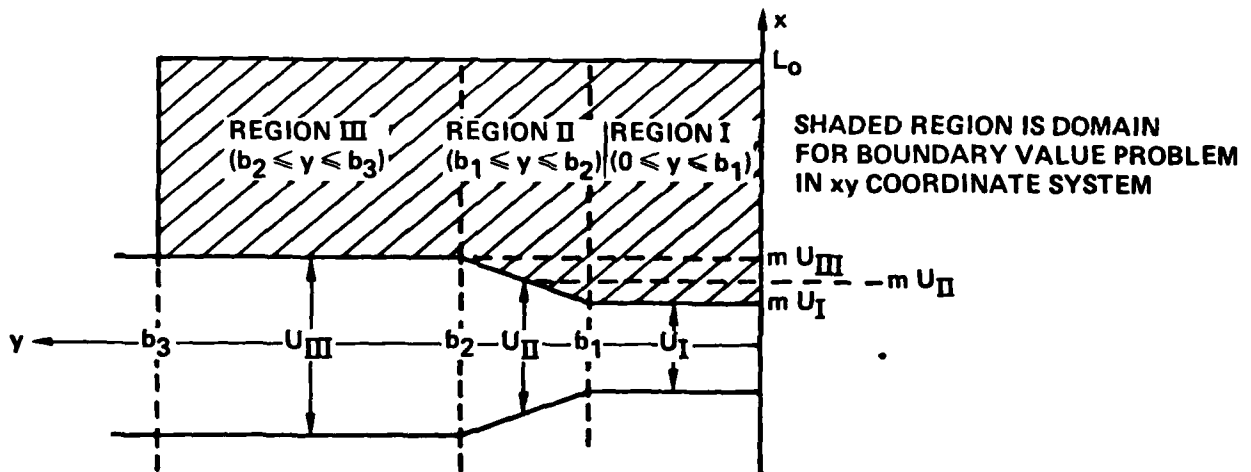
SC80-11378

Figure 1. Definition of Symbols for Three-Region Model of Field Oxidation

In two dimensions the moving boundary is characterized by the function $mU(y,t)$. The above region is mapped into a rectangle by the transformation

$$\xi = \frac{\left[x - mU(y,t)\right]}{L(y,t)} L_I \tag{8a}$$

$$\eta = y \tag{8b}$$

$$\tau = t \tag{8c}$$

where $L(y,t) = L_0 - mU(y,t)$, $L_I = L_0 - mU(y,0) = L_0 - mU_{0I}$, and $U(y,0) = U_{0I} = U_{0II} = U_{0III} = $ constant. Under this transformation the standard two-dimensional nonlinear diffusion equation can be written as

$$\frac{\partial N}{\partial \tau} = \left[\frac{L_I^2 + m^2 U_\eta^2 (L_I - \xi)^2}{L^2}\right] \frac{\partial}{\partial \xi}\left[D(N) \frac{\partial N}{\partial \xi}\right] + \frac{\partial}{\partial \eta}\left[D(N) \frac{\partial N}{\partial \eta}\right]$$

$$- \frac{2mU_\eta}{L}(L_I - \xi) \frac{\partial}{\partial \eta}\left[D(N) \frac{\partial N}{\partial \xi}\right]$$

$$+ \frac{m(L_I - \xi)}{L^2}\left[U_\tau L - (U_{\eta\eta} L + 2mU_\eta^2) D(N)\right] \frac{\partial N}{\partial \xi}$$

$$\text{for } 0 \leq \xi \leq L_I \quad , \quad 0 \leq \eta \leq b_3 \tag{9a}$$

with boundary conditions

$$\frac{\partial N(\xi, 0, \tau)}{\partial \eta} = 0 \qquad ; \qquad 0 \leq \xi \leq L_I \tag{9b}$$

$$\frac{\partial N(\xi, b_3, \tau)}{\partial \eta} = 0 \qquad ; \qquad 0 \leq \xi \leq L_I \tag{9c}$$

$$\frac{\partial N(L_I, \eta, \tau)}{\partial \xi} = 0 \qquad ; \qquad 0 \leq \eta \leq b_3 \tag{9d}$$

$$\left[\frac{L_I D(N)}{L} \frac{\partial N}{\partial \xi}\right]\Bigg|_{\xi=0} + \left[\frac{mU_\eta^2}{L} L_I D(N) \frac{\partial N}{\partial \xi}\right]\Bigg|_{\xi=0} - \left[U_\eta D(N) \frac{\partial N}{\partial \eta}\right]\Bigg|_{\xi=0}$$

$$= (U_\eta^2 + 1)(k - m) U_\tau N(0, \eta, \tau) \qquad ; \qquad 0 \leq \eta \leq b_3 . \tag{9e}$$

The nonlinear diffusion coefficient is selected as that used by Warner and Wilson:[7]

$$D(\gamma) = D^0 \left\{\frac{1 + 19\left[\gamma + \sqrt{\gamma^2 + 1}\right]}{20}\right\} \left[1 + \frac{\gamma}{\sqrt{\gamma^2 + 1}}\right] \tag{9f}$$

where $\gamma = N/2n_{in}$.

As a test case to characterize the moving boundary function $U(\eta, \tau)$, define

$$U_I(\tau) = -(\alpha/2) + \left[\alpha^2/4 + \beta\tau\right]^{\frac{1}{2}} \tag{10a}$$

$$U_{III}(\tau) = 3U_I(\tau) \tag{10b}$$

where α and β are oxide growth parameters in the standard
Deal-Grove model. To interpolate smoothly between these
limits, take

$$U(\eta,\tau) = U_I(\tau) \quad ; \quad 0 \leq \eta \leq b_1 \tag{10c}$$

$$U(\eta,\tau) = U_I + \frac{(U_{III} - U_I)}{b_2 - b_1}(\eta - b_1) - \frac{(U_{III} - U_I)}{2\pi}\sin 2\left[\frac{(\eta - b_1)\pi}{b_2 - b_1}\right]$$

$$b_1 \leq \eta \leq b_2 \tag{10d}$$

$$U(\eta,\tau) = U_{III}(\tau) \quad ; \quad b_2 \leq \eta \leq b_3 . \tag{10e}$$

Although many other selections are possible, this one has
the advantage that U is a continuous function with continuous
first derivative, and that equation (9a) is greatly simplified
in the regions $0 \leq \eta \leq b_1$ and $b_2 \leq \eta \leq b_3$ where $U_\eta = 0$.

3.1.2 Conformal Mapping

The introduction of mixed derivative terms $(\partial^2/\partial\xi\partial\eta)$
into the diffusion equation and the presence of both ξ- and
η-derivatives in the boundary condition at the oxide-silicon
interface are consequences of the lack of orthogonality
between lines of constant ξ and lines of constant η in the
translation-stretching transformation. The impact of these
complications on the efficiency of the numerical procedure
is not small; taken together, they have been found to nearly
triple the CPU time required to obtain a solution.

A simple approach to overcome these difficulties is to employ a conformal map whose level lines closely approximate the desired shape of the silicon region. The construction of appropriate conformal maps for the area beneath a bird's beak oxide layer was studied during FY 1980 under Rockwell IR&D funding; the application of one such mapping to this problem is summarized below.

One can find in standard texts on complex functions[6] the transformation

$$z = \cosh^{-1}\left(\frac{2\zeta - k - 1}{k - 1}\right) - \frac{1}{k}\cosh^{-1}\left[\frac{(k+1)\zeta - 2k}{(k-1)\zeta}\right] , \quad \text{Im } \zeta > 0 , \quad (11)$$

which for $k > 1$ maps the upper half ζ-plane onto a strip with a step in it:

$$\pi(k-1)/k < y < \pi \quad \text{for} \quad x < 0 , \text{ and } \quad 0 < y < \pi \quad \text{for} \quad x \geqslant 0 .$$

Since the exponential transformation $\zeta = e^w$ maps a uniform strip of width π $(0 < \text{Im } w < \pi)$ onto the upper half ζ-plane, the indicated substitution of e^w for ζ in (11) yields a conformal map from a uniform strip to a stepped strip. The exact correspondence is illustrated in Figure 2. A level line $\text{Im } w = \xi_0 > 0$ provides a natural model for the oxide-silicon boundary, the region above ξ_0 corresponding to the silicon layer.

The basic advantage of employing conformal maps is that the structure of neither the differential operator nor its associated boundary conditions is changed thereby. The diffusion equation
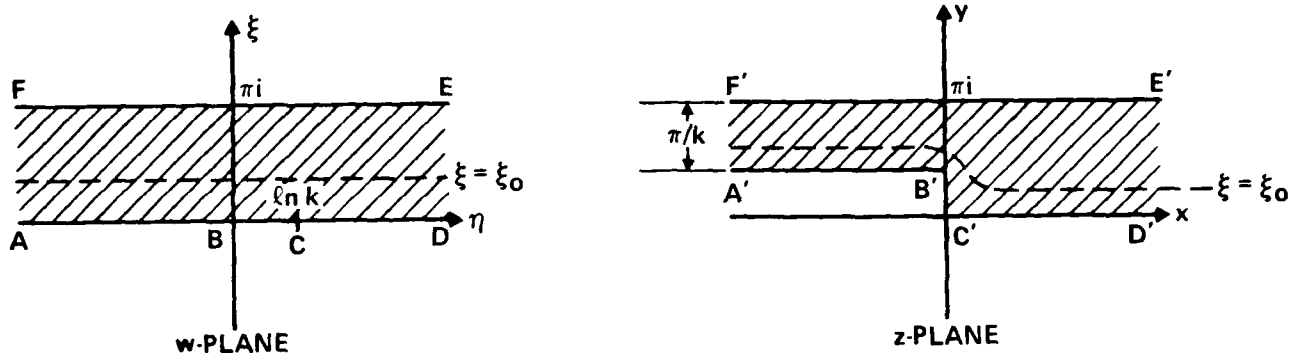
20

Figure 2. Conformal Map from Strip to Stepped Strip:
$w = \eta + i\xi$, $z = x + iy$

$$\frac{\partial}{\partial x}\left(D \frac{\partial N}{\partial x}\right) + \frac{\partial}{\partial y}\left(D \frac{\partial N}{\partial y}\right) = \frac{\partial N}{\partial t} \tag{12}$$

is transformed into

$$\left|\frac{dw}{dz}\right|^2 \left\{\frac{\partial}{\partial \xi}\left(D \frac{\partial N}{\partial \xi}\right) + \frac{\partial}{\partial \eta}\left(D \frac{\partial N}{\partial \eta}\right)\right\} = \frac{\partial N}{\partial \tau} + \frac{\partial N}{\partial \xi}\frac{\partial \xi}{\partial \tau} + \frac{\partial N}{\partial \eta}\frac{\partial \eta}{\partial \tau} , \tag{13}$$

where the time dependence of ξ and η arise from motion of
the oxide-silicon boundary. Using (11), the functions
$\partial \xi/\partial \tau$, $\partial \eta/\partial \tau$, and dw/dz are expressible directly in terms of
ξ, η, and τ, so that computations of dopant diffusion during
oxidation can be carried out on a constant (ξ,η) grid without
reference to physical coordinates. A single transformation
of the dopant profiles to physical coordinates can be
performed after the process cycle is complete.

21

The boundary conditions at the top and bottom of the silicon layer are straightforward to derive, and involve only the normal derivative $\partial N/\partial \xi$. However, the conditions at the lateral edges of the computational domain require some care. If lines $|\eta| = $ constant are chosen to bound this domain, then the physical boundaries in x and y will be somewhat curved, and will change position as the oxide-silicon boundary moves. Fortunately, the effect of conditions at these boundaries on the dopant profiles in the region of interest can be made small by expanding the computational domain laterally. More accurate procedures are available, but are not needed in the present context.

The basic question to be answered with regard to the use of conformal maps for this problem is how large a computational burden is imposed by the necessity to evaluate the functions $\partial \xi/\partial \tau$, $\partial \eta/\partial \tau$, and dw/dz at each time step. This must be compared against the approximate tripling of CPU time experienced with the translation-stretching transformation for the nonuniformly moving boundary problem.

3.2 NUMERICAL PROCEDURES IN TWO SPATIAL DIMENSIONS

3.2.1 B-splines

Although the method of B-splines may be extended to two dimensions, a number of disadvantages make this method noncompetitive with the method of lines. The first difficulty is large storage requirements. For example, using our estimate of a grid of 30×60 with a third order B-spline in each of the two directions, the matrices A (equation (5))

and $\partial F/\partial\alpha$ each have half bandwidth $w = 2 + 2(30 + 2) = 66$.
Because of pivoting requirements, the total storage for both
matrices A and $\partial F/\partial\alpha$ is $s = 2 \times 32 \times 62 \times (3w + 1) = 789{,}632$ words.
If the smaller 20×40 grid with second order B-splines were
adequate, then $w = 21$ and $s = 2 \times 21 \times 41 \times (3w + 1) = 110{,}208$ words.
In either case the storage requirements are excessive.
Secondly, to invert these banded matrices with relatively
large bandwidth many times would require an excessive amount
of computer time. In fact, Warner and Wilson[7] have solved
the easier nonmoving boundary value problem using second
order B-splines on a 21×41 grid and their worst cases
required 7.25 minutes on a Cray-1 computer to integrate to
$t = 0.25$. This translates to at least 36.25 minutes on a
CDC 176 or an IBM 3033*. Finally, the cross derivative term
in equation (9a) may lead to some difficulty because the
existence of Galerkin solutions to such problems have not
completely been determined. Of course, the conformal mapping
formulation doesn't suffer from this disadvantage, but large
storage requirements still limit the B-spline applicability.

---

*Time comparisons between conventional mainframe computers
and the Cray-1 are complicated by the pipeline architecture
of the Cray, which can be used to advantage on large vector
problems. The quoted factor of five above assumes that no
modification of the original FORTRAN code to utilize this
feature was attempted by Warner and Wilson.

3.2.2 Method of Lines

Consider a uniform mesh in the ξ and η direction with meshwidth $\Delta\xi$ and $\Delta\eta$, respectively. For interior points the spatial derivatives in equation (9) are discretized using the following centered difference approximations:

$$\frac{\partial N_{i,j}}{\partial \xi} \approx \frac{N_{i+1,j} - N_{i-1,j}}{2\Delta\xi} \tag{14a}$$

$$\frac{\partial}{\partial \xi}\left[D(N)\ \frac{\partial N}{\partial \xi}\right] \approx D_{i+\frac{1}{2},j}\ \frac{(N_{i+1,j} - N_{ij})}{(\Delta\xi)^2} - D_{i-\frac{1}{2},j}\ \frac{(N_{ij} - N_{i-1,j})}{(\Delta\xi)^2} \tag{14b}$$

$$\frac{\partial}{\partial \eta}\left[D(N)\ \frac{\partial N}{\partial \eta}\right] \approx D_{i,j+\frac{1}{2}}\ \frac{(N_{i,j+1} - N_{ij})}{(\Delta\eta)^2} - D_{i,j-\frac{1}{2}}\ \frac{(N_{ij} - N_{i,j-1})}{(\Delta\eta)^2} \tag{14c}$$

$$\frac{\partial}{\partial \eta}\left[D(N)\ \frac{\partial N}{\partial \xi}\right]$$
$$\approx \frac{D_{i,j+1}(N_{i+1,j+1} - N_{i-1,j+1}) - D_{i,j-1}(N_{i+1,j-1} - N_{i-1,j-1})}{4\Delta\xi\Delta\eta} \tag{14d}$$

where $N_{ij} = N(\xi_i, \eta_j, \tau)$, $D_{ij} = D(N_{ij})$, etc.

Including the boundary conditions, especially equation (9e), leads to very complicated difference expressions. We will merely illustrate the basic idea using one of the second partial derivative terms. Write the first order approximation

24

$$\frac{\partial}{\partial \xi}\left[D(N) \ \frac{\partial N}{\partial \xi}\right] \approx \frac{2}{\Delta\xi}\left[D_{3/2,j} \ \frac{(N_{2,j} - N_{1,j})}{\Delta\xi} - D_{1,j} \ \frac{\partial N_{1,j}}{\partial\xi}\right] \qquad (14e)$$

where the term $\partial N_{1,j}/\partial\xi$ is determined from equation (9e).
In the regions where $U_\eta = 0$, equation (9e) is much simpler
and a discrete version can be written as

$$\frac{\partial N}{\partial \xi} \approx \frac{N_{i+1,j} - N_{i-1,j}}{2\Delta\xi} = \frac{(k - m)U_\tau N_{1j} \cdot L}{L_I D_{1j}} \ . \qquad (14f)$$

The last expression may be solved for $N_{i-1,j}$ and the result
is substituted into equation (14b) to produce a second order
approximation in the regions $0 \leqslant \eta \leqslant b_1$ and $b_2 \leqslant \eta \leqslant b_3$.
Similar techniques are used for the other boundary conditions
and partial derivatives.

As in the one-dimensional case, the spatial variable
differencing leads to a semidiscrete system of nonlinear
ordinary differential equations. The equations corresponding
to the interior mesh points have the form

$$\frac{dN_{i,j}}{d\tau} = f_{i,j}(N_{i,j}, \ N_{i-1,j}, \ N_{i+1,j}, \ N_{i,j+1}, \ N_{i,j-1},$$

$$N_{i+1,j+1}, \ N_{i-1,j+1}, \ N_{i+1,j-1}, \ N_{i-1,j-1}, \ \tau) \ . \qquad (15)$$

Similar equations may be written for the boundary points.
Unfortunately, equation (15) is stiff, and consequently,
the Jacobian, $\partial f/\partial N$, is needed to converge the corrector

equation in the linear multistep method used to solve it.
The coefficient matrix in this Newton-like method is

$$P = I - \Delta\tau\beta_0 \partial f/\partial N \tag{16}$$

where β_0 is a scalar associated with the order of the corrector
equation. Most of the computer time is used in solving the
linear system

$$Px = b . \tag{17}$$

Therefore, it is critical that efficient methods be developed
for solving equation (17). Fortunately, the matrix P need
not be exact but may be approximated by a function which
contains the "basic nature" of the problem being solved.
The consequence of using an approximate Jacobian is that
the iterative procedure may take longer to converge, but
the answer will still be correct. This is analogous to using
the secant method in place of Newton's method when solving
nonlinear equations.

   Two simplifications are made in approximating the Jacobian.
The first is to ignore the cross-derivative term equation (14d)
when evaluating $\partial f/\partial N$ <u>but</u> <u>not</u> <u>when</u> <u>evaluating</u> <u>f</u> (equation (15)).
The rationale in doing this is that the cross-derivative term
is only present in a very small region of the computational
domain ($b_2 \leqslant \eta \leqslant b_3$) where $U_\eta \neq 0$, so that its absence should
not greatly affect the convergence rate. On the other hand,
if this term were present, the solution of equation (17) would
have to be done by the relatively slow banded matrix techniques

26

instead of the much faster iterative methods. The second
simplification assumes that on the boundary $\xi = 0$ and
$b_1 \leqslant \eta \leqslant b_2$ we may write $\partial D/\partial N \approx 0$. There is no real
justification for making this boundary approximation other
than it simplifies the evaluation of the Jacobian. The
price paid for such an approximation is slower convergence.

Applying the above approximations results in a Jacobian
with only 5 nonzero diagonals. Successive overrelaxation
(SOR) methods may be employed to solve equation (17). The
storage problem is minimal, and as P changes from time step
to time step very accurate initial solutions provide fast
convergence. In contrast, banded matrix solvers must start
from scratch each time step and do not use any previous
information.

The numerical solution of (15) is performed by a
variable-order and variable-step-size stiff integrator
similar to the one-dimensional integrator with the critical
equation (17) now being solved by SOR rather than banded
matrix techniques. Our test cases show that this procedure
is superior to the B-spline approach.

3.3 NUMERICAL RESULTS IN TWO DIMENSIONS

The initial condition (ion implant) for the following
test cases is

$$
N(x,y,0) = \begin{cases} \dfrac{N_d \times 10^4}{(2\pi)^{\frac{1}{2}}\sigma_p} \exp\left[-\dfrac{(x-R_p)^2}{2\sigma_p^2}\right] + N_b \; ; \; \begin{array}{l} 0 \leqslant y \leqslant a \\ 0 \leqslant x \leqslant L_0 \end{array} \\[4ex] \dfrac{N_d \times 10^4}{(2\pi)^{\frac{1}{2}}\sigma_p} \exp\left[-\rho^2(y-a)^2\right] \exp\left[-\dfrac{(x-R_p)^2}{2\sigma_p^2}\right] + N_b \; ; \\[3ex] \hspace{5cm} a \leqslant y \leqslant b_3, \; 0 \leqslant x \leqslant L_0 \end{cases}
$$

where σ_p = 0.075 μm, $\rho = \sqrt{2}/\sigma_p$, $N_b = 5 \times 10^{14}$ cm^{-3}, a = $b_3/2$, $N_d = 2 \times 10^{15}$ cm^{-2}, and R_p = 0.285 μm.

In order to determine the lower bounds on computer time, we first consider a nonmoving boundary value problem studied by Warner and Wilson.[7] As noted earlier, their most difficult case required about 36.25 minutes on a CDC 176 to integrate from t = 0 to t = 0.25. Here L_0 = 2.5, b_3 = 5, $U_\tau = U_\eta = 0$, D^0 = 0.0589 μm^2/hr, and $n_i = 9.25 \times 10^{18}$ cm^{-3}. It should be noted that the Jacobian matrix for this problem is <u>exact</u> since no cross derivatives are present in equation (9) and all boundary conditions are homogeneous. Therefore, our computer times should be a minimum for this case. The numerical results are summarized in Table 3 for two computational grids. Here NSTEP denotes the total number of time steps to integrate equation (15). NFE is the number of functional evaluations required of the integrator, i.e., number of times f in equation (15) is evaluated. NJE is the number of times the Jacobian, $\partial f/\partial N$, is evaluated. NII is the total number of internal iterations needed to solve equation (17) by SOR for all time steps up to τ. NQ denotes the present order of the integrator ($1 \leqslant NQ \leqslant 5$). $\Delta\tau$ is the present step size, and CPU denotes the total CPU time in <u>seconds</u> to solve the problem on a CDC 176. These times are remarkably fast compared to those reported by other researchers. Note that the smallest time steps occur between $0 \leqslant \tau \leqslant 0.05$, very few Jacobian evaluations are needed, and the total number of internal iterations (NII) is relatively small.

The initial, as-implemented dopant profile and the result of the quarter-hour drive-in step are shown in

Table 3(a).   11 × 21 Grid

τ	NSTEP	NFE	NJE	NII	NQ	Δτ	CPU (sec)
0.05	32	43	7	77	4	0.0055	
0.10	39	55	8	100	4	0.0085	
0.15	44	63	9	115	4	0.0125	
0.20	48	67	10	123	4	0.0192	
0.25	50	71	10	131	4	0.0192	1.807

Table 3(b).   21 × 41 Grid

τ	NSTEP	NFE	NJE	NII	NQ	Δτ	CPU (sec)
0.05	39	59	8	109	4	0.0040	
0.10	48	70	10	131	4	0.0081	
0.15	54	77	10	145	5	0.0113	
0.20	58	81	10	153	5	0.0113	
0.25	62	86	11	165	5	0.0200	8.217

Figures 3 and 4, respectively. The lateral spread of the boron is quite evident, amounting to a few tenths of a micron. Accurate information of this kind is essential to prediction and control of device electrical characteristics when the overall channel length (separation of source and drain) is of the order of one micron.

For our next degree of difficulty we include a non-uniformly moving boundary with $\alpha = 0.0914$ and $\beta = 0.576$ (equation (10a)), but impose Dirichlet boundary conditions at $\xi = 0$. This will allow us to study the effect of leaving
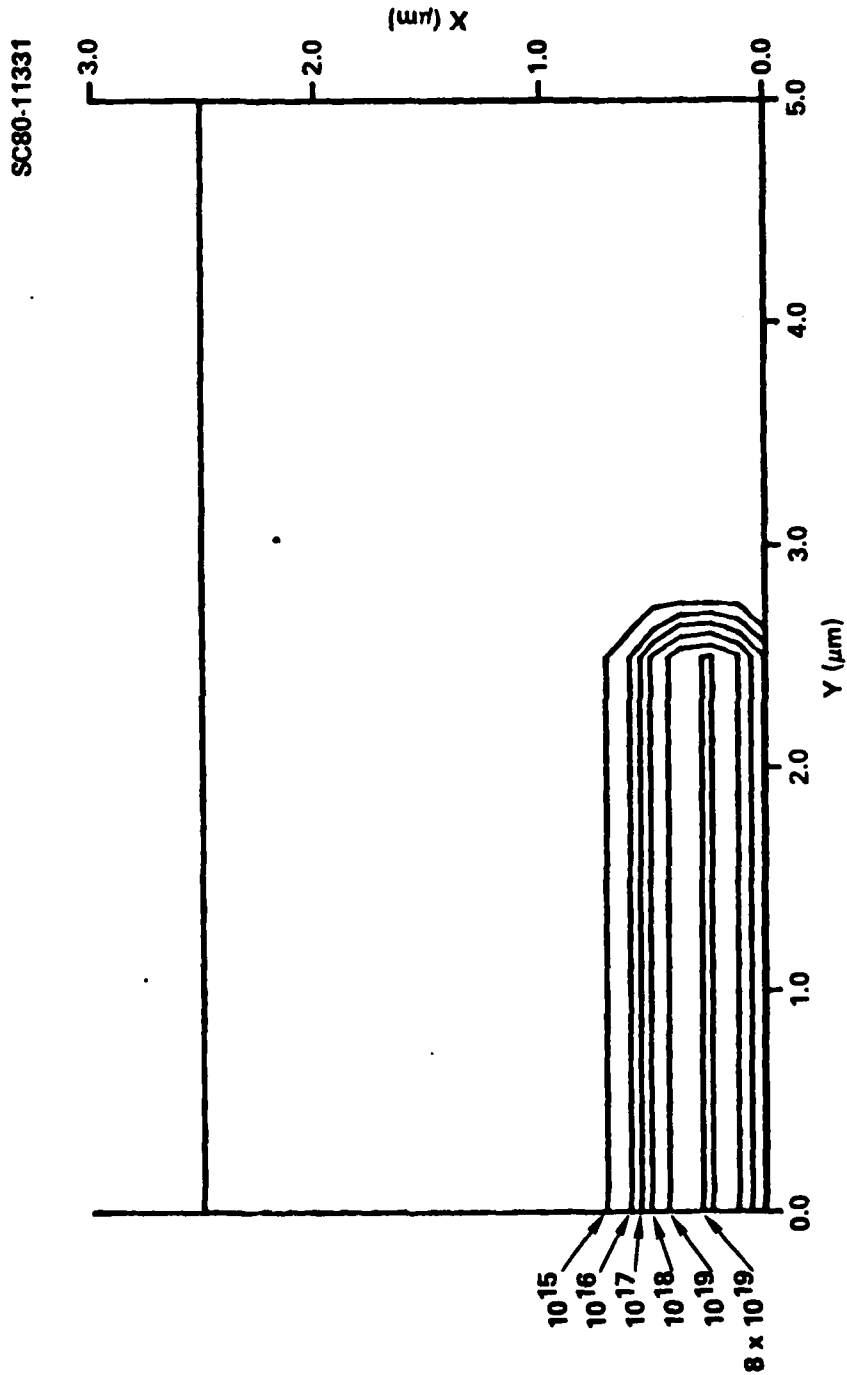
SC80-11331

Figure 3. Contours of Constant Boron Concentration For An 80 keV Implant in (111) Silicon with A Mask Covering The Region y > 2.5 Microns

SC80-11332

X (μm)

3.0

2.0

1.0

0.0

5.0

4.0

3.0

Y (μm)

2.0

1.0

0.0

0.0

10^{15}

10^{16}

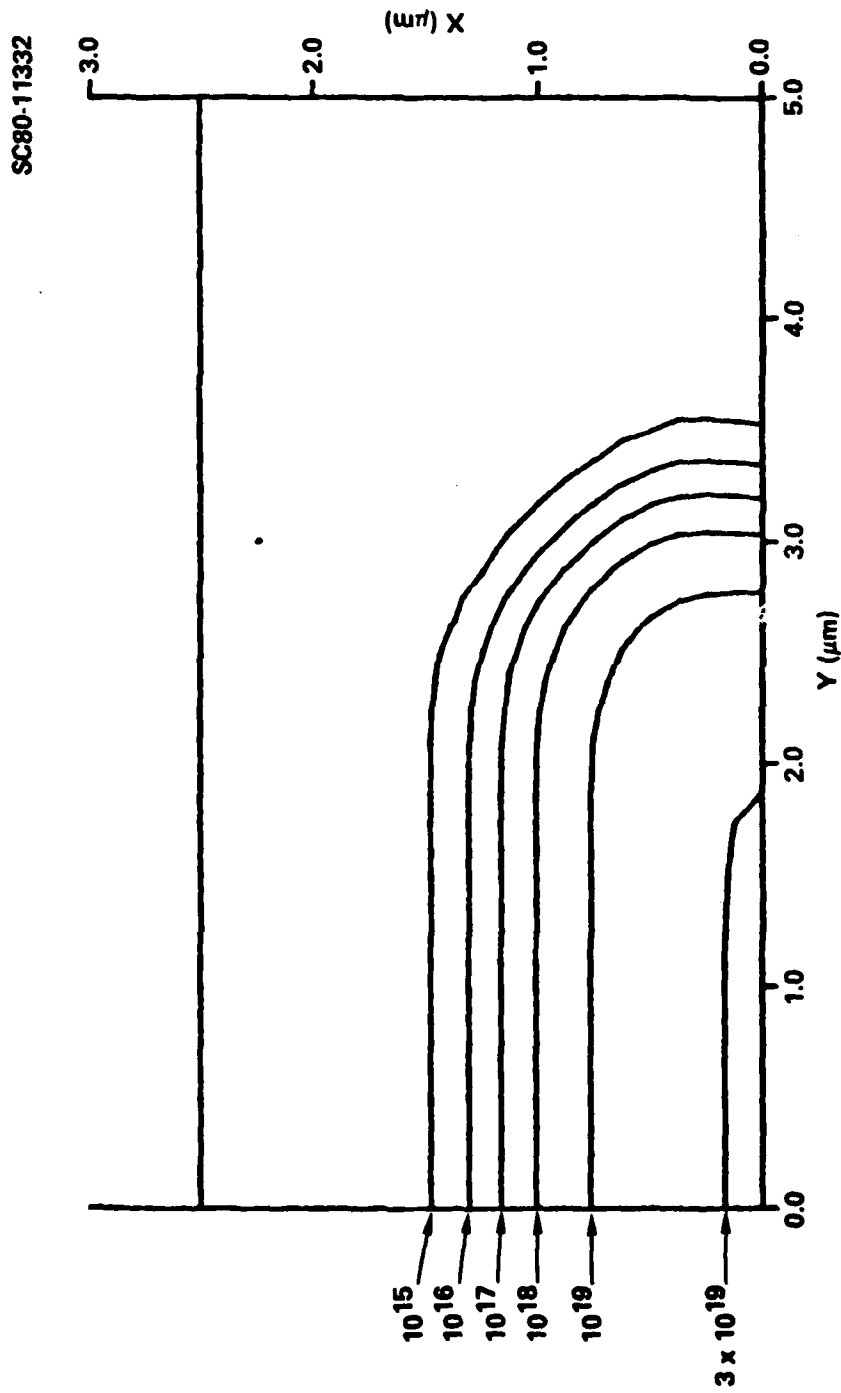10^{17}

10^{18}

10^{19}

3×10^{19}

Figure 4. Redistributed Boron Profile After Subjecting
The Implant of Figure 3 to 1100°C For
15 Minutes in A Non-oxidizing Ambient

31

out the cross-derivative term in the evaluation of the Jacobian. However, the Jacobian of the boundary conditions is still exact. The cross-derivative approximation equation (14d) requires a finer grid, so we set $L_0 = 1.25$ and $b_3 = 2.5$ and use a 21×41 grid. Computational results are given in Table 4. In comparing Table 3(b) with Table 4, we note that the big difference is the number of internal iterations, NII, which is larger when an approximate Jacobian is employed. The integration was carried out to a larger time to allow for a substantial movement of the boundary.

Table 4. Diffusion Equation (9a) with Cross-Derivatives and Dirichlet Boundary Conditions at $\xi = 0$, 21×41 Grid

τ	NSTEP	NFE	NJE	NII	NQ	$\Delta\tau$	CPU (sec)
0.05	55	77	9	155	5	0.0026	
0.10	67	90	11	187	5	0.0055	
0.15	74	98	12	207	5	0.0076	
0.20	80	105	13	229	5	0.0102	
0.25	85	110	13	247	5	0.0126	11.259
0.30	89	116	13	268	5	0.0126	
0.35	93	123	14	296	5	0.0150	
0.40	96	127	14	313	5	0.0150	
0.45	99	132	14	335	5	0.0150	
0.50	103	140	14	371	5	0.0150	16.911

For our final case, we solve equation (9) with a nonuniformly moving boundary and the correct boundary condition (9e). Recall that a second approximation to the Jacobian is used with this boundary condition. The numerical results are illustrated in Table 5. The number of internal iterations is now as much as 65% larger than the previous case. Also, the time steps are smaller. Clearly, the boundary approximation to the Jacobian is a limiting factor on computer time. In the future we will attempt to improve this approximation. Nevertheless, the computer time is quite reasonable for such a difficult problem.

Table 5. Numerical Solution of Equation (9), 21 × 41 Grid

τ	NSTEP	NFE	NJE	NII	NQ	$\Delta\tau$	CPU (sec)
0.05	70	92	10	180	4	0.0022	
0.10	86	112	12	232	4	0.0040	
0.15	97	131	13	288	4	0.0062	
0.20	105	143	13	323	4	0.0074	
0.25	111	157	13	365	4	0.0074	
0.30	118	178	14	428	4	0.0074	
0.35	123	189	15	463	4	0.0099	
0.40	128	204	15	517	4	0.0099	
0.45	134	220	15	574	3	0.0084	
0.50	140	231	16	612	3	0.0084	27.97

4.0 FUTURE WORK

To date, numerical results in two dimensions have been
obtained only for the method of lines algorithm, and nonuni-
form motion of the oxide-silicon boundary has been handled
numerically by the translation-stretching transformation.
We are currently programming the conformal map procedure
outlined in Section 3.1.2 as a potentially faster way to
deal with moving, nonrectangular silicon boundaries typical
of the formation of bird's beak structures in the oxide layer.

In the near term, our emphasis will be on evaluation of
the method of lines algorithm against realistic test cases,
some of which can be solved to known accuracy by other
techniques (e.g., linear diffusion in an impenetrable box).
If time permits, one or two other algorithms which are
potentially very fast will be compared against the method
of lines.

By the end of the first contract year, the speed and
accuracy of the basic algorithm should be well characterized
for typical process steps. The relative merits of different
approaches to the treatment of a nonuniformly moving oxide-
silicon boundary should also be established.

The second year of the contract will be devoted, as
planned, to seeking algorithms for the solution of more
realistic, physically based models for the evolution of
VLSI device structures. Our objective is to provide the
device physicist with computational analysis tools which
can with tolerable speed and accuracy characterize microscopic
processes involving several defect species migrating under

the influence of chemical, mechanical, and electrical driving forces in two (and possibly three) dimensions.

This work will also provide the background for constructing fast algorithms for computer modeling of complete device electrical characteristics based on two-dimensional dopant profiles. While the coupled system of carrier transport and Poisson's equations is considerably more complex than the equations describing multispecies diffusion, there is a strong analogy with the equations governing steady-state fluid flow which can be exploited.

REFERENCES

1. C.D. Maldonado and W.D. Murphy, J. Appl. Phys. 49, 4812 (1978).

2. Carl de Boor, A Practical Guide to Splines, Springer-Verlag (New York, 1978).

3. C.W. Gear, Numerical Initial Value Problems in Ordinary Differential Equations, Prentice-Hall (Englewood Cliffs, N.J., 1971).

4. A.C. Hindmarsh, "GEARB: Solution of Ordinary Differential Equations Having Banded Jacobian," Lawrence Livermore Laboratory UCID-30059, Rev. 1 (March, 1975).

5. J.L. Prince and F.N. Schwettmann, J. Electrochem. Soc. 121, 705 (1974).

6. R.V. Churchill, Introduction to Complex Variables and Applications, McGraw-Hill (New York, 1948).

7. D.D. Warner and C.L. Wilson, Bell System Tech. J. 59, 1 (January, 1980).